



1 **Palaeobiological evidence for Southern Hemisphere Younger**
2 **Dryas and volcanogenic cold periods**

3

4 Richard N Holdaway*^{1,2,3}

5 ¹Palaeocol Research Ltd, P.O. Box 16569, Hornby, Christchurch 8042, New Zealand.

6 ²School of Biological Sciences, University of Canterbury, Private Bag 4800, Christchurch 8041, New Zealand.

7 ³School of Earth and Environment, University of Canterbury, Private Bag 4800, Christchurch 8041, New
8 Zealand.

9

10 *Correspondence to: Richard N. Holdaway (turnagra@gmail.com)

11



12 **Abstract.** Current consensus places a Southern Hemisphere post-glacial cooling episode earlier than the
13 Younger Dryas in the Northern Hemisphere. New Zealand sequences of glacial moraines and speleothem
14 isotopic data are generally interpreted as supporting the absence of a Southern Hemisphere Younger Dryas.
15 Radiocarbon age series of habitat specialist moa (Aves: Dinornithiformes) show, however, that a sudden return
16 to glacial climate in central New Zealand contemporary with the Younger Dryas. The cooling followed
17 significant warming, not cooling, during the period of the Antarctic Cold Reversal. In addition, the moa
18 sequence chronology also shows that the Oruanui (New Zealand) and Mt Takahe (Antarctica) volcanic eruptions
19 were contemporary with abrupt cooling events in New Zealand. The independent high spatial and temporal
20 resolution climate chronology reported here is contrary to an interhemispheric post-glacial climate see-saw
21 model.

22

23

24



25 **1 Introduction**

26 The present model for the interhemispheric relationships between climatic events during the last deglaciation
27 invokes a seesaw alternation of warming with returns to glacial conditions (Broecker, 1998; Barker et al., 2009).
28 The sequence of alternate warming and cooling in each hemisphere model is based predominantly on proxy
29 chronologies from ice and ocean cores and cave speleothems. From these chronologies, post-glacial warming
30 began c.18 ka BP, possibly triggered by a series of eruptions of Mt Takahē (Antarctica) (McConnell et al.,
31 2017), that was reversed temporarily first in the Southern Hemisphere by a cool episode (the Antarctic Cold
32 Reversal, ACR) which, as presently understood, preceded the abrupt return to glacial conditions of the European
33 Younger Dryas between 12.8 ka and 11.5 ka BP.

34 Whether there was a Southern Hemisphere cold period synchronous with the Younger Dryas has been
35 debated for many years, with discussions based partly on data from New Zealand's South Island. The island,
36 athwart the present dominant Southern Hemisphere temperate latitude westerly wind belt, is a key site for
37 Quaternary paleoclimate research. The position and strength of the westerlies has been interpreted from
38 speleothem stable isotopic records and glacial advances and retreats in the axial mountains. These data have
39 been used to both support (Denton & Hendy, 1994; Ivy-Ochs et al., 1999) and reject (Shulmeister et al., 2005;
40 Hajdas et al., 2006; Kaplan et al., 2010; Koffman et al., 2017; Putnam et al., 2010) a New Zealand Younger
41 Dryas episode. The moraines, speleothems, and pollen as climate proxies provide overviews of atmospheric and
42 conditions through time but they are either contentious, as with the origin of the Waihō Loop (Denton & Hendy,
43 1994; Mabin et al., 1996; Tovar et al., 2008), or, with speleothem isotopes and pollen, have been recovered from
44 relatively few sites, and are subject to different interpretations (Newnham, 1999; Singer et al., 1998). All,
45 especially the Kaipo Bog pollen record (Lowe & Hogg, 1986; Hajdas et al., 2006), depend on date-interpolated
46 stratigraphic chronologies. In addition, apart from rare instances such as the Kaipo Bog, the sites do not record
47 local environments in detail through space and time.

48 In contrast, the rich radiocarbon record for moa (Aves: Dinornithiformes), whose late Holocene
49 distributions indicate high levels of habitat specificity, provides a geographically extensive, independent,
50 intensive chronology of vegetation, west of the Main Divide (MD), in the western and northwestern South
51 Island, New Zealand over the past 25,000 years (Worthy, 1993a; Worthy, 1997; Worthy & Holdaway, 1993,
52 1994; Worthy & Roscoe, 2003). I used the published radiocarbon ages of four moa taxa characteristic of
53 alpine/glacial, lowland rain forest, and dry shrublands to develop a chronology of vegetation change through
54 time, comparable with interpretations of local speleothem $\delta^{18}\text{O}$ palaeotemperature records and the European



55 Younger Dryas chronology from ice accumulation, temperature (Meese et al., 1994)) and methane (Brook et al.,
56 1996) records over the past 30 ka from the GISP2 ice core (Greenland).

57

58 **2 Materials and methods**

59 **2.1 Geographic settings**

60 **2.1.1 West Coast, South Island**

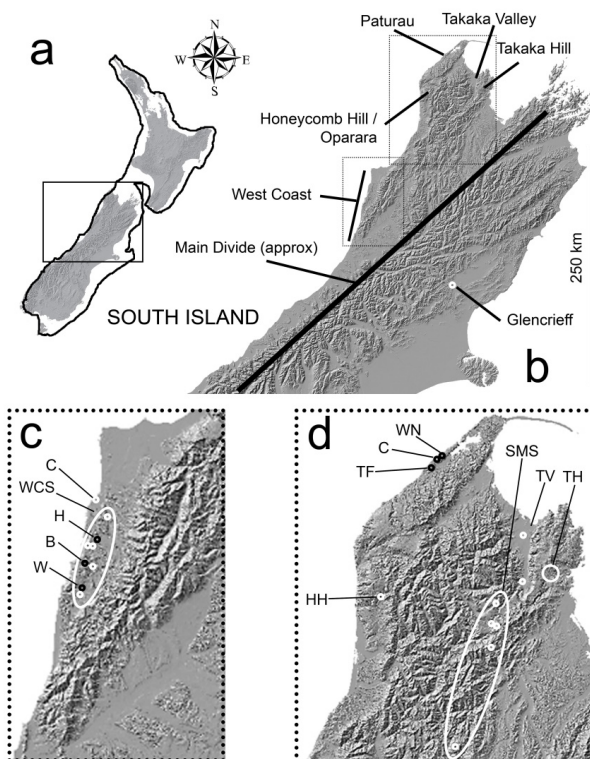
61 The West Coast fossil sites are within caves and cave systems in the 6000 ha of karst that abuts the coast south
62 of Charleston (Fig. 1). The area is bounded to the east by the 1500 m Paparoa Range. The limestone is c. 100 m
63 thick so there is little vertical development in the caverns, but horizontal passages can be up to 8 km long
64 (Worthy & Holdaway, 1993). The sites vary in present altitude from 10s to 300 m above sea level. The present
65 climate is mild, humid, and equable, with mean summer maxima of c. 18°C and minima of c. 10 °C (Worthy &
66 Holdaway, 1993). The dominant westerly winds bring precipitation from the Tasman Sea and beyond. Rainfall
67 varies from 2800 mm at the coast to 4000 mm at the base of the eastern ranges, with 8000 mm at the summit.
68 Annual sunshine hours range from 1700 in the south to nearly 2000 in the north. Fed by the ample moisture and
69 mild temperatures the Holocene vegetation has been lowland rain forest, with podocarp conifers emergent above
70 a canopy of broadleaf trees and an understory of shrubs and tree ferns.

71

72 **2.1.2 Honeycomb Hill**

73 The Honeycomb Hill Cave system of 13.7 km of passages, with 70 entrances, lies beneath 0.8 km² of temperate
74 rain forest (Worthy, 1993a) in the broad, shallow Oparara River basin in the north-western South Island (Fig. 1).
75 The basin is sheltered, and normally experiences only light winds, mostly from the west. Annual rainfall is
76 3000-4000 mm (Worthy, 1993a). Frosts are uncommon and temperatures are similar to those in the West Coast
77 study area. The present altitude of 300 m a.s.l. was c. 430 m during the glacial maximum.

78



79

80 **Figure 1:** Distribution of fossil deposits and speleothems in the northern South Island, New Zealand. Fossil
81 deposits, black; speleothem sites, white. **A,** Location of study area in relation to present and Last Glacial
82 Maximum (solid line) coastlines. **B,** Western and northwestern study areas and Glencrieff site in relation to the
83 Main Divide. **C,** Detail of West Coast study area. C, Charleston; WCS, West Coast fossil sites; H, Hollywood
84 Cave; B, Babylon Cave; W, Wasspretti Cave. **D,** Detail of Northwest Nelson study area. WN, Wet Neck Cave;
85 C, Creighton's Cave; TF, Twin Forks Cave; HH, Honeycomb Hill Cave system; SMS, Southern mountain sites;
86 TV, Takaka Valley; TH, Takaka Hill; A, Mt Arthur (Nettlebed Cave)

87

88 2.1.3 Takaka Hill

89 Takaka Hill (TH) is a roughly tear-drop-shaped (in plan) complex of ranges and marble plateaux which projects
90 40 km north from the high (1500-1800 m) mountainous core of northwest Nelson (Fig. 1). The southern end is a
91 narrow saddle reaching 1000 m, between the headwaters of the Waitui Stream to the west and the South Branch



92 of the Riwaka River to the east, which pinches it off from the southern mountains. The ‘Hill’ itself, c. 20 km
93 across at its widest point, is therefore in effect an island, bounded by steep escarpments to the east and west and
94 to the north (during the Holocene) by the sea. The western escarpment is the boundary with Takaka Valley (TV)
95 where there are fossil deposits in limestone caves: to the east the abrupt slopes fall to the Waimea Plains (Fig.
96 1), which have great depths of alluvium and no known Quaternary fossil deposits. Most of the fossil sites on TH
97 are presently at 800-900 m above sea level, but would have been up to 1000 m during the glaciation.

98 Although at present near sea level, TV would have been near 250 m at Last Glacial Maximum. During
99 the Weichselian-Otiran glaciation TH and TV were near the center of the larger glacial period New Zealand land
100 mass, much farther than at present from coastal and marine influences. To the north, extensive lowlands of the
101 land bridge occupied the western reaches of present Cook Strait. The land bridge allowed contact, at times,
102 between the faunas and floras of the North and South islands. The status of the Cook Strait land bridge as
103 alternatively a barrier to movement or a conduit has been much debated, e.g., (Worthy, 1993b; Worthy &
104 Holdaway, 1994).

105 Its roles as barrier or conduit probably changed with extrinsic events. For example, the Oruanui
106 eruption of Taupo Volcano 25.6 ka BP (Vandergoes et al., 2013) would have deposited thick ash on the bridge
107 (Vandergoes et al., 2013), destroying the vegetation (Oppenheimer, 2011), and making it uninhabitable by moa
108 or anything else. Under the cold, dry glacial climate revegetation would have taken millennia.

109 Much of the forest on TH was removed in the early 20th century. Surviving patches indicate that the
110 Holocene mixed forest was dominated by *Fuscospora* and *Lophozonia* southern beeches (both formerly in
111 *Nothofagus*) with emergent podocarps including *Podocarpus totara* and *P. laetus* (formerly *P. hallii* or *P.*
112 *cunninghamii*) (Worthy & Holdaway, 1994). The Holocene TV rain forest was much floristically richer than
113 that on TH. Rainfall in TV and on TH is high and TH regularly receives (southern) winter snow.

114

115 **2.1.4 Glencrieff**

116 The Glencrieff site (Fig. 1) (Worthy & Holdaway, 1996) is a small bog formed over a spring in a grazed field on
117 a gravel river terrace c. 1.6 km west of the well-known Pyramid Valley lake bed deposit (Holdaway & Worthy,
118 1997; Holdaway et al., 2014; Allentoft et al., 2014). The moa remains lay within a 1.2 m peat layer beneath the
119 turf. The peat in turn overlays fluid blue clay over a gravel base at c. 2.5 m. Pollen recovered from the peat



120 suggested that the local vegetation during moa deposition was tussock grasses (mostly *Chionochloa* spp.) with
121 the small conifer *Phyllocladus alpinus* and *Coprosma* spp. shrubland. As both *Chionochloa* and *Coprosma* are
122 both anemophilous and produce large amounts of mobile pollen, they may be over-represented in the deposit.

123

124 **2.1.5 Merino Cave, Annandale**

125 Merino Cave is at the foot of the slope in a small doline at 560 m at the southern end of a limestone plateau in
126 North Canterbury which rises to Mt Cookson (897 m) (Fig. 1). To the west, the eastern axial mountain ranges
127 reach >1700 m. The moa remains were excavated, with those of other birds, from the sides and floor of a
128 channel cut through a sediment fill (Worthy & Holdaway, 1995).

129

130 **2.2 Systematics – nomenclature of *Pachyornis* and *Euryapteryx***

131 It is necessary for clarity to briefly summarize recent changes in moa nomenclature because older major reviews
132 such as (Worthy & Holdaway, 2002) use older names and even species definitions. In *Pachyornis*, the validity
133 of *P. australis* was accepted on its morphology by (Worthy, 1989) and confirmed genetically later (Bunce et al.,
134 2009). Further analyses of the distributions and relationships of taxa within South Island *Pachyornis* led
135 (Rawlence et al., 2012) to question the validity of some identifications based on morphology. From this, and
136 stable isotope measurements, (Holdaway & Rowe, 2020) suggested that only *P. australis* was found west of the
137 Main Divide. For the present analysis, *Pachyornis* individuals west of the MD are treated as *P. australis*.
138 However, the distinctions detailed by (Rawlence et al., 2012) are followed below completeness.

139 In the genus *Euryapteryx*, re-examination of a type specimen necessitated name changes. *E. curtus* was
140 known until 2005 as *E. geranoides*. It was then renamed *E. gravis* (Worthy, 2005). Four years later it was
141 incorporated in an expanded concept of *E. curtus* (Bunce et al., 2009). However, the systematics of the genus
142 appear to be still not settled as two sympatric genetic clades of different body sizes from the Holocene of the
143 northern North Island's northern peninsula have been referred to as different species (Huynen et al., 2010) or
144 subspecies (Huynen et al., 2014). They are unlikely to have been subspecies as the forms were sympatric and
145 contemporary. The *Euryapteryx* specimens are listed provisionally here as *E. curtus*.

146



147

148 **2.3 Habitat specificity of moa**

149 **2.3.1 General**

150 The key observation that allows some moa to be used as vegetation proxies is that those taxa have been found
151 only in association with specific vegetation types in deposits of Holocene age. The Holocene vegetation pattern
152 is well known from existing examples and many pollen records.

153 South Island moa were formerly characterized in terms of “faunas”, principally with respect to a
154 distinction between Holocene age “eastern” and “western” faunas (Worthy & Holdaway, 1993, 1994, 1996,
155 2002). The western “wet forest” fauna was based on the presence of *Anomalopteryx* and smaller individuals of
156 *Dinornis robustus*. Mid-sized individuals of *D. robustus* in western deposits were then identified as a separate
157 species (*D. novaezealandiae*) characteristic of wet forests. The eastern fauna was based on the presence of
158 *Euryapteryx* and *Pachyornis*. These genera have been seen as characteristic of dry shrubland/forest mosaics (Worthy,
159 2000; Holdaway & Worthy, 1997; Worthy & Holdaway, 1994, 1996). Another emeid moa, *Emeus crassus*, was
160 also characteristic of the eastern fauna but it has never been identified in deposits west of the MD (Worthy
161 & Holdaway, 2002), so provides no vegetation information for that area.

162 As noted above, these distinctions and the habitat preferences of the moa taxa were based on the
163 Holocene vegetation, which is well known both from surviving vegetation and pollen records. Habitat
164 requirements recognised here for the key taxa follow.

165 **2.3.2 *P. australis***

166 This species indicates the presence of shrublands growing under a cool to cold climate. It occupied alpine
167 shrublands and fellfield in the Holocene (Worthy, 1989; Rawlence & Cooper, 2013; Worthy & Holdaway, 1994;
168 Rawlence et al., 2012), and is hypothesized to have occupied similar habitat during glaciations. The youngest
169 radiocarbon dated individuals are from higher altitudes than *P. elephantopus* (Rawlence & Cooper, 2013;
170 Rawlence et al., 2012).

171

172

173



174 2.3.3 *Anomalopteryx didiformis*

175 This small species indicates the presence of warm lowland to lower montane rain forest (Worthy & Holdaway,
176 1993, 1994, 2002). Carbon stable isotope ratios suggest that it fed around canopy gaps within the rain forest
177 (Worthy & Holdaway, 2002).

178 2.3.4 *Euryapteryx curtus*

179 This species is found in Holocene in areas of lowland to lower montane dry forest and shrublands (Worthy &
180 Holdaway, 2002). It is here taken to indicate the presence of such vegetation and also of seral vegetation with
181 similar structure and composition.

182

183 **2.4 Moa radiocarbon ages**

184 **2.4.1 Sources**

185 Radiocarbon ages for moa obtained from the literature are listed, with ancillary data, in Tables 1 & 2. Those
186 from the South Island West Coast are from (Worthy & Holdaway, 1993, 1994; Bunce et al., 2009); from
187 Honeycomb Hill from (Worthy, 1993a; Rawlence et al., 2012; Bunce et al., 2009); from Glencrieff from
188 references (Worthy & Holdaway, 1996; Rawlence et al., 2011); from Takaka Valley and Takaka Hill from
189 (Worthy & Holdaway, 1994; Worthy & Roscoe, 2003; Rawlence et al., 2012; Bunce et al., 2009). Those from
190 Annandale are in (Worthy & Holdaway, 1995).

191

192 **2.4.2 Radiocarbon age calibration**

193 All conventional radiocarbon ages were calibrated using OxCal4.4 (Ramsey, 2009) referenced to the SHCal20
194 curve (Hogg et al., 2020). The dates are presented as means or as means $\pm 1\sigma$. At the chronological scales
195 involved, symbol size in the figures generally encompasses the probability distribution for calibrated dates.

196

197

198

199



200 **2.5 Bayesian sequence analyses**

201 Sequences of moa radiocarbon ages and the timing of changes in representation were assessed using the
202 R_Sequence option in OxCal4.3 (Ramsey, 1995, 2009), again invoking the SHCal20 curve (Hogg et al., 2020).
203 Sequence starts and ends were plotted both as means and standard deviations and as probability distributions.

204 **2.6 Isotopes and other proxies**

205 Palaeoclimatic data were downloaded from the National Climatic Data Center of the National Oceanographic
206 and Atmospheric Administration (NOAA) www.ncdc.noaa.gov. The speleothem $\delta^{18}\text{O}$ data are from (Hellstrom
207 et al., 1998), (Williams et al., 2005) and (Williams et al., 2010). Data for GISP2 ice accumulation are from
208 (Meese et al., 1994) and for GISP2 methane from (Brook et al., 1996).

209 Isotope, methane, and ice accumulation data were smoothed using local regression (LOESS), via the
210 LOESS option in PAST® (Hammer et al., 2001). A range of smoothing factors (Fig. 2-4) was tested to establish
211 which showed the best compromise between loss of pattern and excessive noise: a common smoothing factor of
212 0.03 was adopted. At all SF values, the fall in temperature signaled by the 8-speleothem $\delta^{18}\text{O}$ record coincided
213 with the start of the Younger Dryas in Greenland (Fig. 4).

214

215 **2.7 Eruption dates**

216 The date of the Oruanui (Taupo) super eruption is from radiocarbon ages in (Vandergoes et al., 2013)
217 recalibrated using the SHCal20 curve. The Mt Takahe eruption series date, based on Antarctic ice core
218 chronologies, is from (McConnell et al., 2017). The Mt Takahe eruptions coincided with a peak of warming
219 shown in the New Zealand $\delta^{18}\text{O}$ record, immediately preceding a return to low temperatures, rather than being at
220 the start of local warming (Fig. 2, 3).

221

222

223



224 **Table 1:** Conventional and calibrated (SHCal20 curve) radiocarbon ages (Before Present) for moa from West Coast,
225 Honeycomb Hill, Glencrieff, and Merino Cave deposits, South Island, New Zealand. *, Site 16 is also known as
226 Equinox Cave; NP, not published; ANDI, *Anomalopteryx didiformis*; PAEL, *Pachyornis elephantopus*; PAAU, *P.*
227 *australis*; PAAU, *P. australis* identified as *P. elephantopus* on morphology; EUCU, *Euryapteryx curtus*; EMCR,
228 *Emeus crassus*. Ages in italics, ANU laboratory series with different pretreatments (Rawlence et al., 2011).
229 Calibrated dates in square parentheses, failed χ^2 test for combination. Date laboratory numbers in **bold** used in
230 sequence analysis. N/A, not available. References: B, Bunce *et al.* (2009); R11, Rawlence *et al.* (2011); R12,
231 Rawlence *et al.* (2012); W93, Worthy (1993a); W&H 93, Worthy & Holdaway (1993); W&H 95, Worthy &
232 Holdaway (1995); W&H 96, Worthy & Holdaway (1996).



Taxon	Museum	Site	Lab no.	CRA	SD	Cal mean	SD	Median	Reference
WEST COAST									
ANDI	NMNZ S28055-61	Madonna Cave Sites 1-8	NZA2443	2197	86	2193	114	2141	W & H 93
PAEL	NMNZ S28064	Madonna Cave Site 8	NZA2505	14740	110	17985	164	18008	W & H 93
PAEL	NMNZ S28086	Madonna Cave Site 14	NZA2446	20680	160	24846	234	24861	W & H 93
PAAU	NMNZ S28192	Te Ana Titi Cave	NZA2320	25070	260	29360	308	29345	W & H 93
EUCU	NMNZ S28083	Madonna Cave Site 13	NZA2779	11090	100	12971	101	12977	W & H 93
EUCU	NMNZ S28121	Madonna Cave Site 16*	NZA2445	23780	210	27964	249	27924	W & H 93
PAAU	CMAv29445	Charleston	OxA12431	14045	65	17054	122	17043	B
HONEYCOMB HILL CAVE SYSTEM									
PAAU	<i>In situ</i>	Gradungula Passage	OxA12435	18925	80	22786	126	22800	B
PAAU	<i>In situ</i> , NRS348	Gradungula Passage	OxA20284	19575	80	23526	144	23517	R 12
PAAU	<i>In situ</i> , NRS350	Gradungula Passage	OxA20285	20760	90	24979	141	24998	R 12
PAAU	NMNZ S25863.2	Moa Cave Extension	OxA20366	17645	60	21254	131	21257	R 12
PAAU	NMNZ S25863.1	Moa Cave Extension	OxA20367	19335	70	23262	190	23210	R 12
PAAU	NMNZ S25655	Wren Wrecker	OxA20286	16860	75	20336	99	20344	R 12
PAAU	NMNZ S25868	Cemetery	ANU1611	14730	170	17922	238	17953	R 12
PAAU	NMNZ S25867	Cemetery	ANU1612	14950	150	18240	218	18220	R 12
PAAU	NMNZ S25864	Cemetery	NZ7646	15000	200	18292	257	18283	W 93
PAAU	N/A	Graveyard	NZ6586	14029	138	16995	212	17005	W 93
PAAU	N/A	Graveyard	NZ6453	15677	163	18953	180	18940	W 93
PAAU	N/A	Graveyard	NZ7323	18600	230	22531	243	22520	W 93
PAAU	N/A	Graveyard	NZ7292	20600	450	24773	528	24767	W 93
PAAU	N/A	Moa Cave	NZ7642	13850	140	16746	211	16752	W 93
PAAU	N/A	Moa Cave	NZ6480	14194	140	17234	203	17222	W 93
PAAU	N/A	Moa Cave	NZA574	18300	170	22185	186	22199	W 93
PAAU	N/A	Moa Cave	NZ7647	18650	250	22577	256	22572	W 93
PAAU	N/A	Moa Cave Extension	NZ6589	14062	138	17047	209	17055	W 93
PAAU	N/A	Cemetery	NZ7675	12950	450	15391	722	15403	W 93
GLENCRIEFF									
PAEL	NP	Glencrieff "Peg 1"	NZA4162	11898	82	13722	115	13709	W & H 96
PAEL	NMNZ 32670.9	Glencrieff Square A1	ANU1607	11230	210	13106	193	13106	R 11
	NMNZ 32670.9	Glencrieff Square A1	ANU4923	10750	80	12682	69	12698	R 11
	NMNZ 32670.9	Glencrieff Square A1	ANU7612	10510	80	12377	177	12384	R 11
	Combined					12645	64	12658	
PAEL	NMNZ S32670.8	Glencrieff Square A2	ANU4937	9070	80	10161	135	10192	R 11
	NMNZ S32670.8	Glencrieff Square A2	ANU7265	10680	70	12637	74	12654	R 11
	Combined					[11561]	144	11563	
PAEL	NMNZ S32670.3	Glencrieff Square A1	ANU1606	11490	80	13337	81	13337	R 11
	NMNZ S32670.3	Glencrieff Square A1	ANU4925	11180	70	13063	78	13077	R 11
	NMNZ S32670.3	Glencrieff Square A1	ANU7614	10980	70	12880	83	12869	R 11
	Combined					[13109]	45	13111	
PAEL	NMNZ S32670.7	Glencrieff Square B2/B3	ANU7610	11390	130	13260	116	13256	R 11
PAEL	NMNZ S32670.2	Glencrieff Square B2	ANU1605	10580	90	12487	169	12529	R 11
	NMNZ S32670.2	Glencrieff Square B2	ANU4924	10760	70	12694	57	12707	R 11
	NMNZ S32670.2	Glencrieff Square B2	ANU7613	10610	80	12554	130	12583	R 11
	Combined					12640	61	12654	
EMCR	NMNZ S32690	Glencrieff – Square A1	NZA4079	10470	130	12289	225	12296	W & H 96; R 11
EMCR	NMNZ S32688	Glencrieff – Square A1	NZA4018	10480	120	12307	213	12312	W & H 96; R 11
ANNANDALE									
PAEL	NMNZ33402-3pt	Merino Cave - West	NZA3814	14150	140	17174	208	17176	W & H 95
PAEL	NMNZ33402-3pt	Merino Cave - West	NZA3815	19580	230	23503	262	23500	W & H 95
PAEL	NMNZ33402-3pt	Merino Cave - East	NZA3816	38200	980	42422	630	42378	W & H 95
PAEL	NMNZ33402-3pt	Merino Cave - East	NZA3884	22690	400	26901	403	26918	W & H 95
PAEL	NMNZ33402-3pt	Merino Cave - East	NZA4197	37820	810	42144	455	42157	W & H 95
PAEL	NMNZ33402-3pt	Merino Cave - East	NZA4447	14010	110	16974	181	16982	W & H 95

233

234

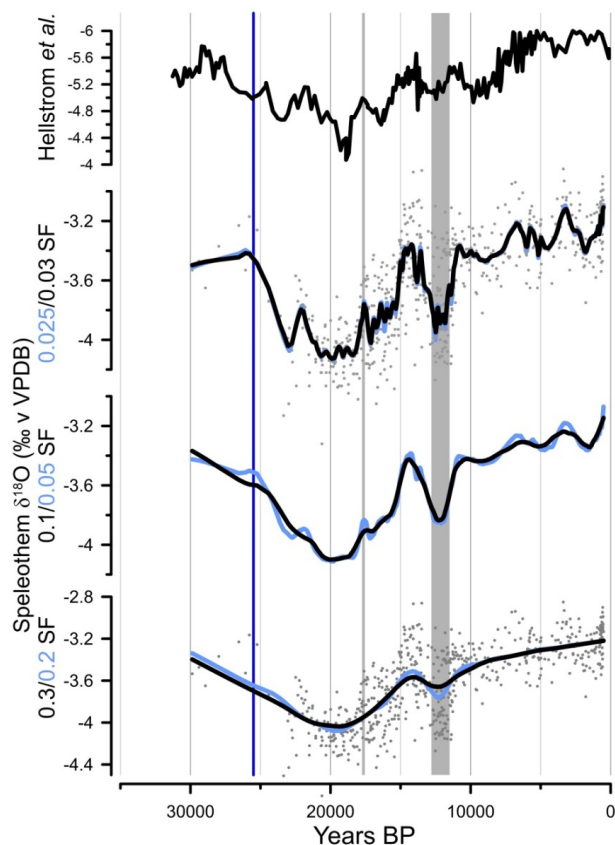


235
 236
 237
 238

Table 2: Radiocarbon ages for moa from the Takaka area, north-western South Island, New Zealand. References: B, Bunce et al. (2009); R, Rawlence *et al.* (2012); W & H 94, Worthy & Holdaway (1994); W & R 03, Worthy & Roscoe (2003).

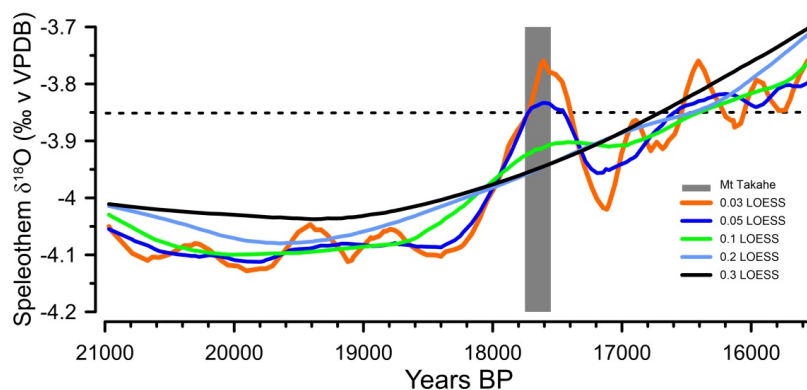
Taxon	Museum	Site	Lab no.	CRA	SD	Cal mean	SD	Median	Reference
ANDI	NMNZ S38943	Takaka Fossil Cave	OxA12728	11575	45	13406	52	13407	B
ANDI		Takaka Fossil Cave	NZA11614	11354	60	13223	55	13221	W & R 03
ANDI		Kairuru Extension	NZA3288	8274	72	9217	114	9213	W & H 94
ANDI		Hawkes Cave	NZA3258	6656	141	7500	127	7503	W & H 94
ANDI		Kairuru Extension	NZA3289	4072	59	4544	117	4524	W & H 94
ANDI		Takaka Fossil Cave	NZA13547	1576	60	1429	65	1425	W & R 03
ANDI		Irvine's Tomo	NZA3048	670	59	604	39	604	W & H 94
EUCU		Takaka Valley	NZA3050	14080	100	17096	154	17093	W & H 94
EUCU		Takaka Valley	NZA3051	13889	95	16805	153	16813	W & H 94
EUCU		Takaka Hill	NZA1567	13400	130	16083	196	16082	W & H 94
EUCU	S39016	Takaka	OxA12670	12525	50	14698	188	14677	B
EUCU		Takaka Fossil Cave	NZA13267	12450	65	14563	206	14547	W & R 03
EUCU		Takaka Fossil Cave	NZA13266	12361	65	14407	223	14349	W & R 03)
PAELN	S32425	Predator Cave	OxA20336	32230	380	36616	441	36579	R
PAAU	S28422	Hawkes Cave	NZA3237	29011	312	33392	484	33444	W & H 94
PAELN	DM417E	Takaka Hill	OxA20292	20330	90	24390	143	24386	R
PAEL	S27797	Kairuru	NZA1568	18950	230	22836	271	22815	W & H 94
PAAU	NM unreg	Takaka Hill	OxA20290	18235	80	22160	92	22160	R
PAELN	DM417E	Takaka Hill	OxA20293	14145	60	17184	93	17183	R
PAEL	S28424	Hawkes Cave	NZA3240	13470	94	16178	150	16179	W & H 94
PAAU	S33754	Moa Trap Cave	OxA12669	10450	45	12303	136	12299	B
PAAU	WO90.47	Takaka Hill	OxA20291	10210	45	11814	89	11822	R
PAAU	Av21331	Bone Cave	OxA12430	10165	50	11716	134	11745	B
PAAU	S27881	Irvine's Tomo	NZA3049	28520	290	32687	470	32669	W & H 94
PAAU	S35298.1	Commentary Cave	OxA20294	28050	300	32151	465	32062	R
PAEL	NMNZ	Tarakohe	NZA3047	19520	130	23466	189	23472	W & H 94

239



240
241
242
243
244
245
246
247
248
249

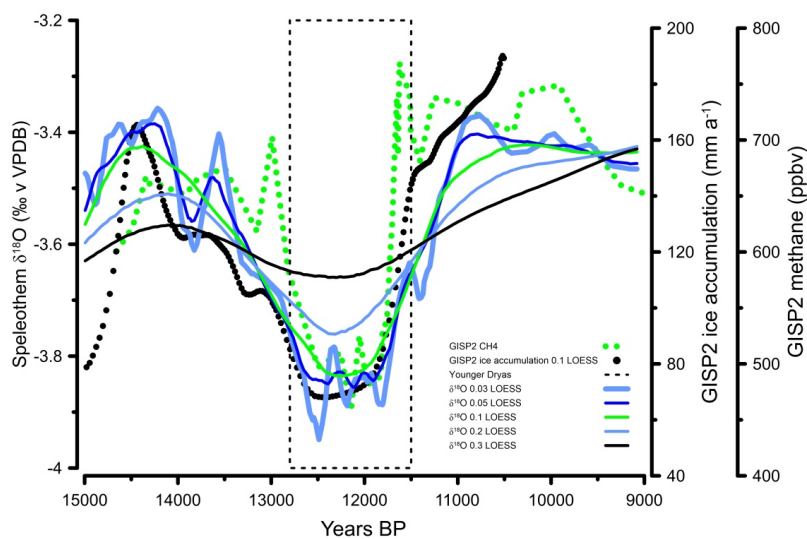
Figure 2: Effects of different smoothing factors on full sequence of speleothem $\delta^{18}\text{O}$ records in western and northwestern South Island, New Zealand. **A**, speleothem MD1, Mt Arthur. **B**, Integrated speleothem records from eight caves near Paturau and on the West Coast, South Island, New Zealand; grey symbols, raw data; black, local regression (LOESS) 0.03 smoothing factor (SF) (adopted for analyses); blue = 0.025 SF. **C**, As in B but black = 0.1 SF, blue = 0.05 SF; **D**, As in B, black = 0.3 SF, blue = 0.2 SF. Line at 25.6 ka BP, Oruanui (Taupo volcano, New Zealand, eruption); at 17.7 ka BP, Mt Takahe, Antarctica, eruption series. Grey shading, European Younger Dryas.



250

251 **Figure 3:** Effects of different smoothing factors (SF) on LOESS (local regression) of the 8-speleothem integrated
252 $\delta^{18}\text{O}$ record for the north-western South Island in the period encompassing the Mt Takahe (Antarctica) eruptions.
253 0.03 SF adopted for further analyses.

254



255

256 **Figure 4:** As in Fig. 3, but for the period encompassing the North Hemisphere Younger Dryas, in relation also to
257 GISP2 ice core methane and ice accumulation records (with 0.1 SF).

258

259

260



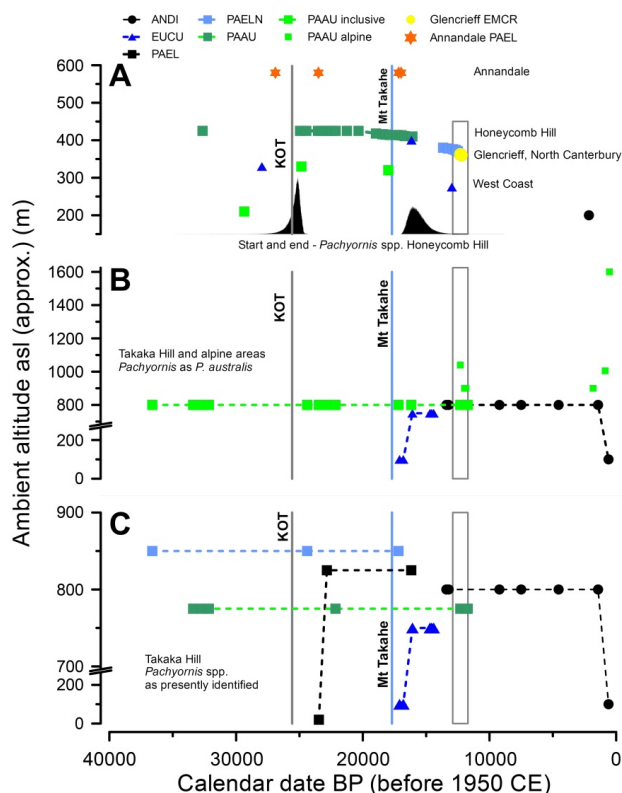
261 **3 Results**

262 Analysis of radiocarbon ages on bone gelatin of moa from cave sites at different altitudes in the north-western South
263 Island, New Zealand, and a swamp site (Glencrieff) and cave site (Merino Cave, Annandale) east of the Main
264 Divide showed changes in species representation in relation to each other, to the Oruanui super eruption (Taupo,
265 New Zealand) and Mt Takahe eruptions (Antarctica), and to the period of the Younger Dryas (Fig. 5-8; Tables 1-3).

266 East of the MD, a population of *Pachyornis elephantopus* around Glencrieff was replaced by *Emeus*
267 *crassus* at the onset of the Younger Dryas (Fig. 5, 6; Table 3), but both taxa were present in the area later in the
268 Holocene (Holdaway et al. 2014). Only individuals of *Pachyornis* have been dated so far from Merino Cave. They
269 were present around the time of the Oruanui eruption and after the Mt Takahe eruptions. West of the MD, apart
270 from an individual > 30 ka old, deposition of *Pachyornis australis* in the Honeycomb Hill cave system began
271 immediately after the Oruanui eruption (Fig. 5, 7; Table 4). Further south, in the West Coast area, two of the three
272 available ¹⁴C ages on *P. australis* fell immediately after the Oruanui and immediately before the Mt Takahe
273 eruptions (Fig. 5A). The third, from a site at lower altitude, pre-dated the Oruanui eruption. One of the two available
274 ¹⁴C ages on *Euryapteryx curtus* from the West Coast pre-dated the Oruanui eruption; the other coincided with the
275 start of the Younger Dryas (Fig. 5A). Despite significant numbers of *Anomalopteryx didiformis* in West Coast sites,
276 only one, with a late Holocene age, has been ¹⁴C-dated so far. Its presence was then assumed to indicate its presence
277 in the Holocene only (Worthy & Holdaway, 1993).

278 Further north, ¹⁴C ages for *P. australis*, *E. curtus*, and *A. didiformis* from Takaka Hill and the mountains to
279 the south were clustered (Fig. 5B, C). Taking all the *Pachyornis* individuals as representing *P. australis* (Holdaway
280 & Rowe, 2020), the species exhibited four pulses of presence on Takaka Hill (Fig. 5B). The first, at 38-34 ka BP,
281 included the date for the single pre-Oruanui individual from Honeycomb Hill. As at Honeycomb Hill, there was a
282 pulse of deposition after the Oruanui eruption, then none after 22 ka BP until after the Mt Takahe eruptions (Fig.
283 5B). *P. australis* was then replaced briefly by *A. didiformis* during the Antarctic Cold Reversal interval, only to
284 return in the Younger Dryas period (Fig. 5, 8; Table 5). It vanished from Takaka Hill between 11.59 ka and 11.23 ka
285 BP, synchronous with the end of the Younger Dryas (Fig. 5, 8; Table 5), after which it remained at higher altitudes
286 in the mountains to the south, until its extinction (Fig. 5B). The *Pachyornis* individuals arrayed as presently
287 identified (*P. australis*, *P. elephantopus* northern clade, *P. elephantopus (sensu lato)*) appear sequentially in the
288 Takaka area after both eruptions (Fig. 5C).

289
290



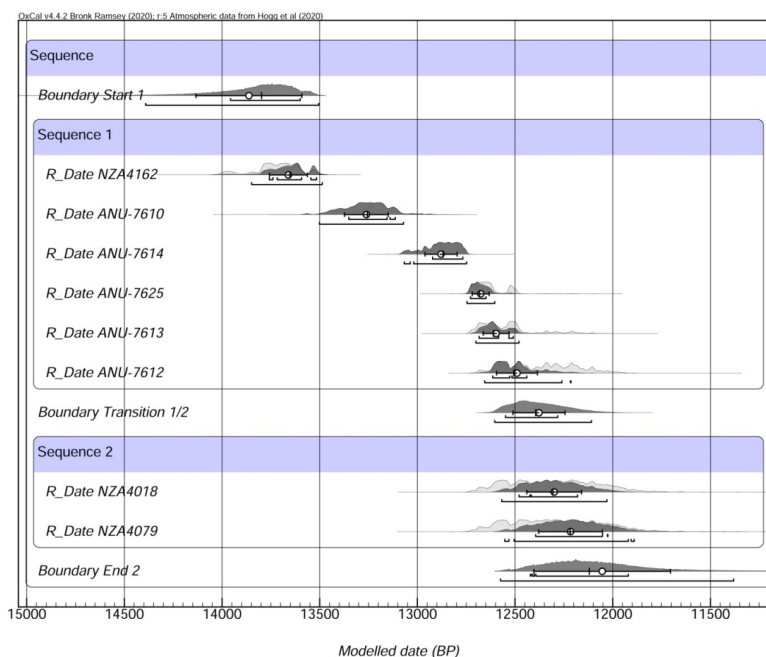
291
 292
 293
 294
 295
 296
 297
 298
 299
 300
 301

Figure 5: Species sequences of moa in the northern South Island, New Zealand over the past 40,000 years in relation to the Oruanui and Mt Takaha eruptions and the Younger Dryas and to ambient altitude above sea level (asl). Mean calibrated dates for moa in: A, the Honeycomb Hill cave system, the West Coast, and Glencrieff, with Bayesian probabilities (shaded) of start and end of deposition of *Pachyornis australis* at Honeycomb Hill; B, the Takaka area, all *Pachyornis* regarded as *P. australis*; and C, the Takaka area with *Pachyornis* as presently identified. Abbreviations: KOT, Oruanui eruption; ANDI, *Anomalopteryx didiformis*; EUCU, *Euryapteryx curtus*; PAEL, *Pachyornis elephantopus* sensu lato; PAELN, *P. elephantopus*, northern clade; PAAU, *P. australis* as presently identified; PAAU inclusive, all *Pachyornis* west of the Main Divide regarded here as *P. australis*.



302
303

304



305 **Figure 6:** Bayesian modelled dates for transition between presence of *Pachyornis elephantopus* and *Emeus crassus*
306 in the Glencrieff deposit, eastern South Island, New Zealand.

307

308 Currently, there are no ¹⁴C-dated *E. curtus* from the Takaka area from earlier than the Mt Takahe eruptions
309 (Fig. 5B). The short date series begins with individuals in the Takaka Valley, adjacent to the main part of the Cook
310 Strait land bridge (Fig. 8B), and only later on Takaka Hill, where its final date just precedes the brief presence of *A.*
311 *didiformis* itself just preceding the period of the European Younger Dryas.

312 Features in the moa date series and sequences aligned with the 8-speleothem $\delta^{18}\text{O}$ paleotemperature
313 records and with both ice

314
315



320 9A). Two other features of the 8-speleothem curve of note are a sudden drop at the time of the Oruanui
321 eruption (Fig. 9A), and a steep rise starting c. 18 ka BP, peaking at the Mt Takahe eruptions before falling
322 and not reaching the same value again until c. 15 ka BP (Fig. 9B, 10). Neither feature appears in the GISP2
323 ice accumulation curve.

324 Bayesian sequence analysis indicated that deposition of *P. australis* ceased at Honeycomb Hill two
325 centuries after the post-glacial rise in $\delta^{18}\text{O}$, at c. 3.85‰ (Fig. 9, 10). The species reappeared at c. 17.4 ka BP,
326 as $\delta^{18}\text{O}$ fell below c. 3.85‰ (Fig. 10) and persisted until c. 16.5 ka BP. The gap in presence of *P. australis* in
327 the Honeycomb Hill record bracketed the Mt Takahe eruptions, ceasing as the climate warmed and returning
328 as it cooled immediately after the eruptions.

329 The smoothed local $\delta^{18}\text{O}$ and GISP2 curves showed similar patterns before and after the Younger
330 Dryas (Fig. 9, 11). *Anomalopteryx didiformis* appeared briefly on Takaka Hill before the Younger Dryas,
331 indicating that rain forest had reached at least 800 m a.s.l. during the post-glacial warming. It was then
332 replaced on Takaka Hill during the European Younger Dryas period (Fig. 9, 11). *A. didiformis* reappeared in
333 the early Holocene (Fig. 9, 11).

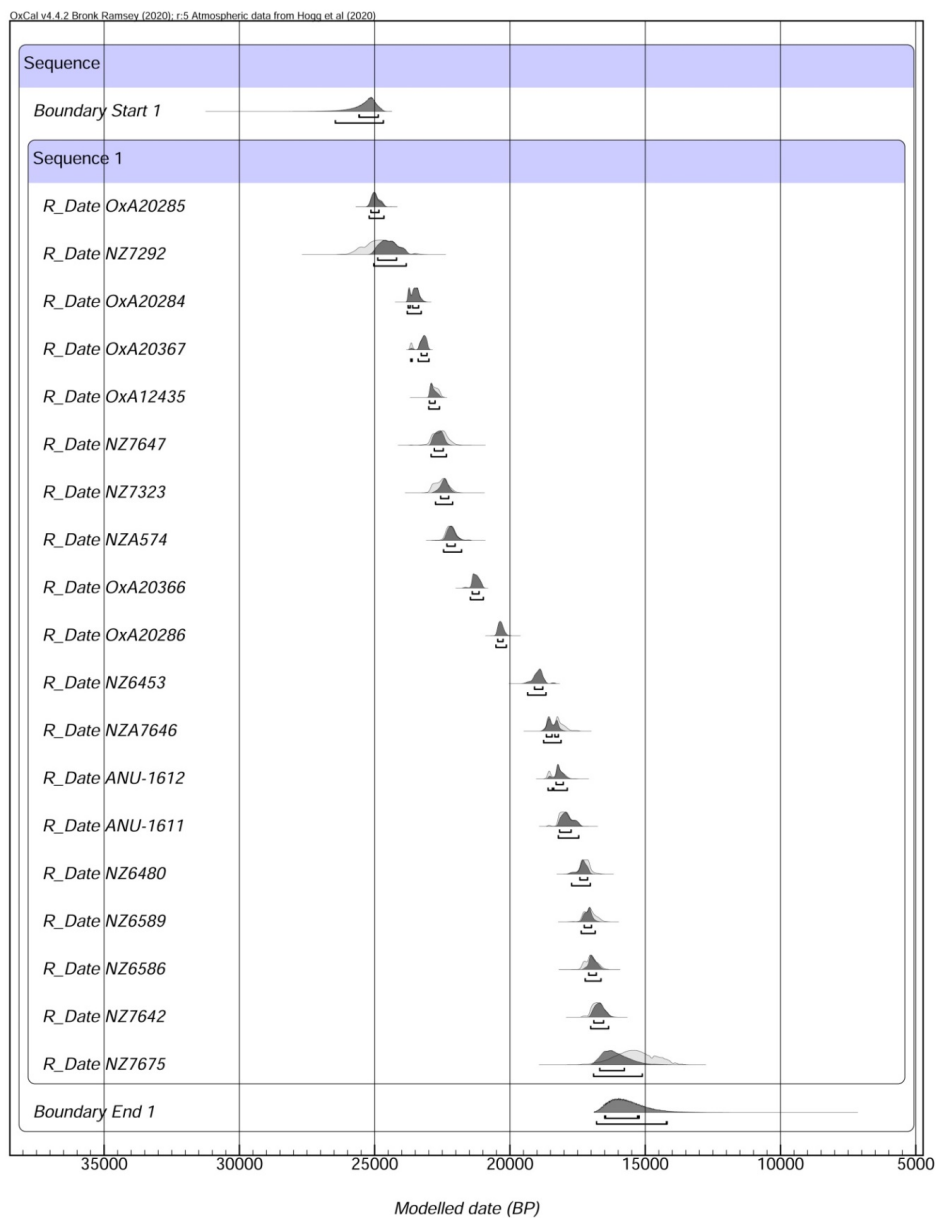
334



Name	Unmodelled (BP)										Modelled (BP)										Indices						
	from	to	%	from	to	%	from	to	%	from	to	%	from	to	%	from	to	%	μ	σ	m	Y	A _{model} =124.8	A _{overall} =122.3	A _{comb} A		
Post KOT sequence																											
Show structure																											
Curve SHCal20																											
Sequence																											
Boundary Start 1	Arrival of <i>P. australis</i>																										
Sequence 1																											
R_Date OxA20285	25156	24886	68.3	25220	24679	95.4	24979	141	24998	25139	24842	68.3	25202	24656	95.4	24952	146	24973	4.5	96.1	25271	25271	4.5	96.1			
R_Date NZ7292	25275	24185	68.3	25775	23815	95.4	24773	528	24767	24881	24186	68.3	25031	23831	95.4	24461	328	24482	4.5	108.4							
R_Date OxA20284	23760	23366	68.3	23793	23250	95.4	23522	150	23515	23763	23376	68.3	23795	23281	95.4	23538	146	23530	4.5	101.5							
R_Date OxA20367	23317	23053	68.3	23710	23003	95.4	23262	190	23210	23279	23065	68.3	23664	22993	95.4	23206	133	23186	4.5	108							
R_Date OxA12435	22956	22690	68.3	22991	22551	95.4	22786	126	22800	22974	22767	68.3	23000	22605	95.4	22833	109	22857	4.5	107.4							
R_Date NZ7647	22867	22359	68.3	23022	22066	95.4	22577	256	22572	22796	22466	68.3	22914	22347	95.4	22625	153	22625	4.5	116.3							
R_Date NZ7323	22810	22305	68.3	22973	22079	95.4	22531	243	22520	22560	22265	68.3	22750	22120	95.4	22423	153	22418	4.5	112.3							
R_Date NZA574	22372	22051	68.3	22528	21776	95.4	22185	186	22199	22330	22028	68.3	22453	21788	95.4	22141	171	22159	4.5	101.7							
R_Date OxA20366	21395	21141	68.3	21463	20984	95.4	21254	131	21257	21395	21142	68.3	21463	20984	95.4	21254	131	21258	4.5	100							
R_Date OxA20286	20451	20257	68.3	20516	20134	95.4	20336	99	20344	20451	20256	68.3	20516	20134	95.4	20336	99	20344	4.5	99.9							
R_Date NZ6453	19096	18784	68.3	19384	18655	95.4	18953	180	18940	19094	18787	68.3	19350	18667	95.4	18962	169	18944	4.5	101.4							
R_Date NZA7646	18639	18063	68.3	18756	17806	95.4	18292	257	18283	18654	18210	68.3	18754	18110	95.4	18442	175	18475	4.5	108.9							
R_Date ANU-1612	18599	18020	68.3	18647	17868	95.4	18240	218	18220	18296	18031	68.3	18591	17880	95.4	18191	160	18192	4.5	112							
R_Date ANU-1611	18222	17782	68.3	18268	17422	95.4	17922	238	17953	18166	17742	68.3	18213	17458	95.4	17870	207	17900	4.5	100.9							
R_Date NZ6480	17382	17047	68.3	17766	16861	95.4	17234	203	17222	17417	17133	68.3	17721	17032	95.4	17318	166	17302	4.5	102.2							
R_Date NZ6589	17315	16900	68.3	17400	16616	95.4	17047	209	17055	17253	16986	68.3	17365	16849	95.4	17107	132	17101	4.5	117.7							
R_Date NZ6586	17281	16818	68.3	17377	16585	95.4	16995	212	17005	17086	16808	68.3	17218	16635	95.4	16934	143	16947	4.5	112.6							
R_Date NZ7642	16988	16564	68.3	17114	16293	95.4	16746	211	16752	16901	16543	68.3	17015	16354	95.4	16695	173	16701	4.5	106							
R_Date NZ7675	16161	14551	68.3	16840	14029	95.4	15391	722	15403	16672	15764	68.3	16910	15100	95.4	16081	486	16158	4.5	82.4							
Boundary End 1	<i>P. australis</i> extirpation																										
	16467 15200 68.3 16804 14158 95.4 15634 712 15755 4.5																										

327

328 **Table 4:** Bayesian results for dates of moa species succession at Honeycomb Hill, Oparara, South Island, New Zealand.



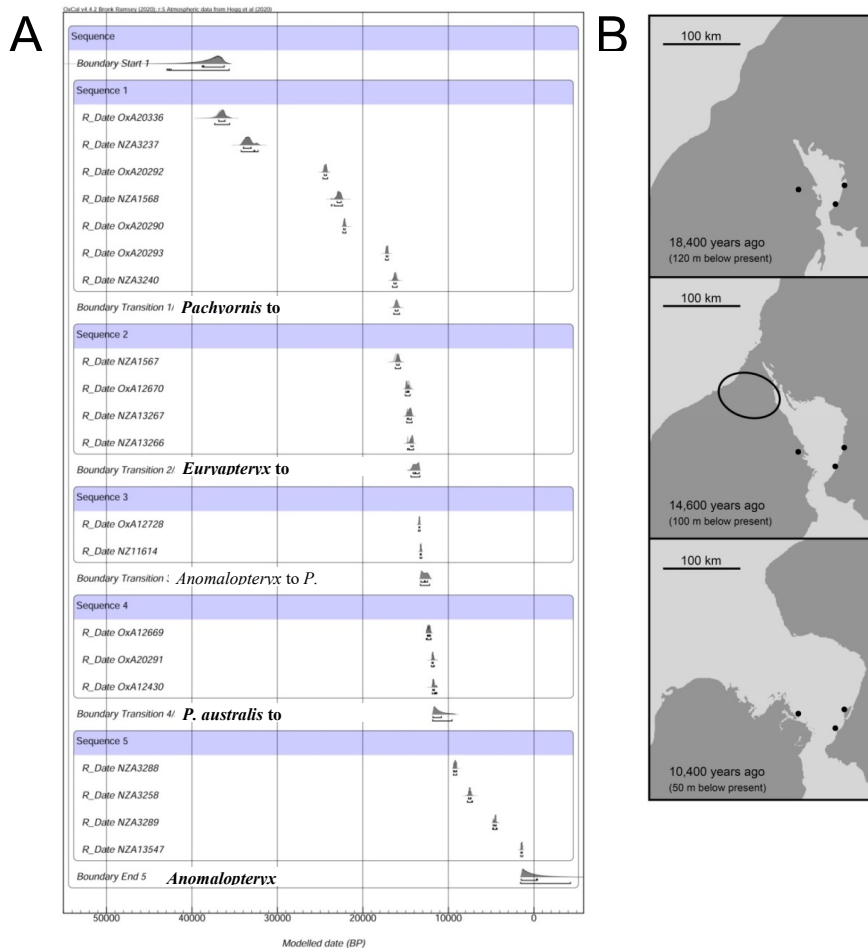
337
338 **Figure 7:** Bayesian modelled dates for the first and last *Pachyornis australis* after 30 ka BP in deposits in
339 the Honeycomb Hill Cave system, South Island, New Zealand.

340
341



Name	Unmodelled (BP)										Modelled (BP)										Indices	
	from	to	%	from	to	%	μ	σ	m	A	from	to	%	from	to	%	μ	σ	m	A	$A_{model}=103.2$	$A_{unmodel}=102.8$
Show all																						
Show structure																						
Curve SHCal20																						
Boundary Start 1	First <i>Pachyornis</i>																					
Sequence 1																						
R_Date OxA20292	24532	24242	68.3	24672	24123	95.4	24390	143	24386	143	24386	24505	24218	68.3	24657	24101	95.4	24366	143	24357	99.8	
R_Date NZA1568	23015	22530	68.3	23679	22367	95.4	22836	271	22815	23014	22529	68.3	23675	22368	95.4	22837	271	22815	100.1			
R_Date OxA20290	22254	22068	68.3	22345	21980	95.4	22160	92	22160	22254	22068	68.3	22345	21980	95.4	22160	92	22160	100.1			
R_Date OxA20293	17278	17069	68.3	17359	17025	95.4	17184	93	17183	17277	17069	68.3	17358	17025	95.4	17184	93	17182	99.9			
R_Date NZA3240	16320	16030	68.3	16489	15870	95.4	16178	150	16179	16380	16108	68.3	16547	15994	95.4	16259	139	16254	96.8			
Boundary Transition 1/2	<i>P. australis</i> to <i>E. curvius</i>																					
Sequence 2																						
R_Date NZA1567	16275	15884	68.3	16480	15699	95.4	16083	196	16082	16064	15750	68.3	16225	15598	95.4	15902	158	15901	86.1			
R_Date OxA12670	14958	14514	68.3	15015	14322	95.4	14698	188	14677	14980	14602	68.3	15049	14475	95.4	14791	158	14838	105.3			
R_Date NZA13267	14831	14319	68.3	14941	14201	95.4	14563	206	14547	14821	14325	68.3	14880	14255	95.4	14550	172	14529	107.9			
R_Date NZA13266	14791	14125	68.3	14837	14076	95.4	14407	223	14349	14383	14120	68.3	14781	14072	95.4	14312	155	14280	109.4			
Boundary Transition 2/3	<i>E. curvius</i> to <i>A. dufiformis</i>																					
Sequence 3																						
R_Date OxA12728	13458	13352	68.3	13496	13313	95.4	13406	52	13407	13454	13347	68.3	13493	13312	95.4	13402	51	13401	100.1			
R_Date NZ11614	13296	13167	68.3	13316	13108	95.4	13223	55	13221	13298	13170	68.3	13320	13110	95.4	13227	54	13226	99.8			
Boundary Transition 3/4	<i>A. dufiformis</i> to <i>P. australis</i>																					
Sequence 4																						
R_Date OxA12669	12477	12099	68.3	12594	12063	95.4	12303	136	12299	12472	12094	68.3	12585	12019	95.4	12276	135	12271	98.4			
R_Date OxA20291	11925	11735	68.3	11975	11525	95.4	11810	103	11820	11926	11780	68.3	11987	11651	95.4	11848	71	11850	106.4			
R_Date OxA12430	11872	11635	68.3	11930	11343	95.4	11716	134	11745	11839	11636	68.3	11883	11345	95.4	11706	119	11733	105			
Boundary Transition 4/5	<i>P. australis</i> to <i>A. dufiformis</i>																					
Sequence 5																						
R_Date NZA3288	9398	9032	68.3	9421	9021	95.4	9217	114	9213	9397	9032	68.3	9420	9020	95.4	9216	114	9212	100			
R_Date NZA3258	7658	7340	68.3	7777	7180	95.4	7500	127	7503	7658	7357	68.3	7776	7182	95.4	7500	127	7503	99.9			
R_Date NZA3289	4780	4417	68.3	4818	4301	95.4	4544	117	4524	4781	4417	68.3	4818	4303	95.4	4544	117	4523	99.8			
R_Date NZA13547	1514	1359	68.3	1538	1310	95.4	1429	65	1425	1516	1365	68.3	1540	1309	95.4	1433	65	1431	99.4			
Boundary End 5																						
333																						
334																						
335																						

Table 5. Bayesian results for dates of moa species succession in the Takaka area, South Island, New Zealand.



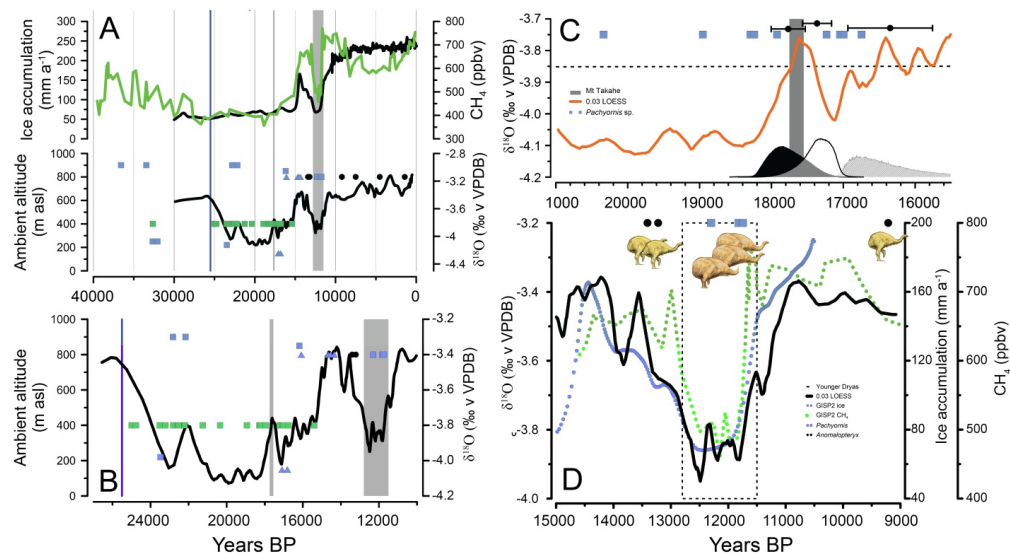
343
 344
 345
 346
 347
 348
 349
 350

Figure 8: Bayesian modelled dates for transitions between moa taxa in the Takaka area, South Island, New Zealand and their geographic context. **A**, Bayesian modelled transition dates. **B**, Extent of the Cook Strait land bridge and when it was severed by rising post-glacial sea level. Bathymetric data from New Zealand Hydrographic Charts: NZ46, Cook Strait Narrows, 1:200000, published Jan 1989, Hydrographer RNZN. New Edition 2000, Land Information New Zealand; NZ48, Cook Strait Western Approaches, 1:400000, published Apr 1998, Hydrographer RNZN. New Edition Apr 2000, Land Information New Zealand.



351
352

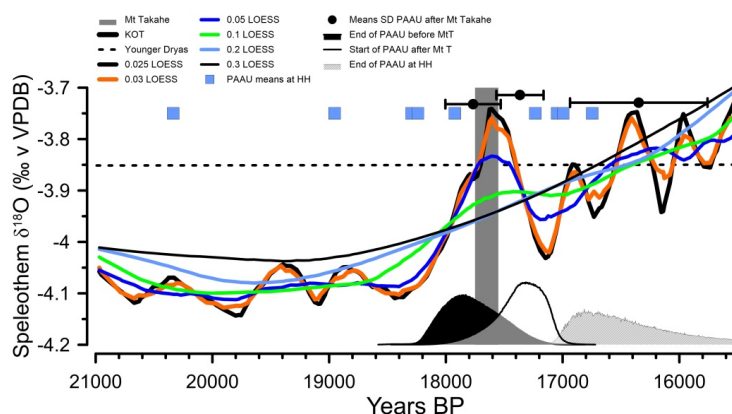
353



354
355

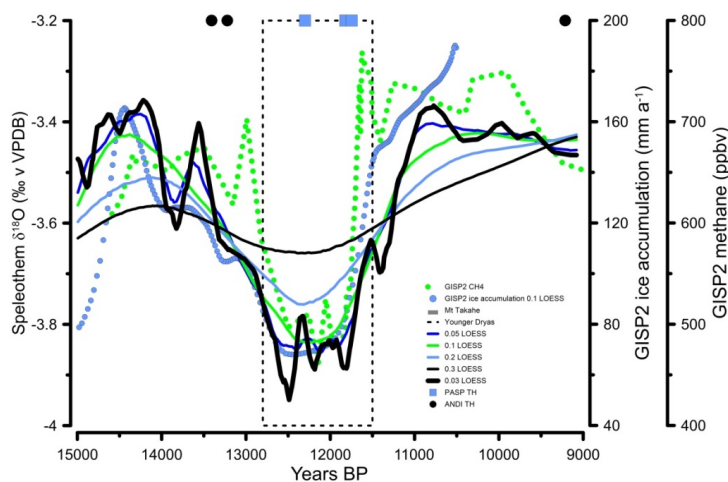
Figure 9: Moa taxa responded to the Younger Dryas climate shifts and volcanic events by tracking the resulting geographic and altitudinal changes in their habitats. **A**, comparison of GISP2 (Greenland) ice accumulation (black) and methane (green) (upper curves) with (lower curve) integrated speleothem $\delta^{18}\text{O}$ records for the northwestern South Island and mean calibrated dates for moa at Honeycomb Hill and near Takaka. Vertical lines, L-R: Oruanui eruption; Mt Takahe eruptions; Younger Dryas. **B**, detail of moa dates in comparison with northwestern South Island speleothem $\delta^{18}\text{O}$. **C**, detail of dates for *Pachyornis australis* at Honeycomb Hill in relation to $\delta^{18}\text{O}$ record and period of Mt Takahe (Antarctica) eruptions (shaded bar). Bayesian modelled dates for end of *P. australis* presence before Mt Takahe, resumption of presence post-Mt Takahe, and extirpation of *P. australis* at Honeycomb Hill indicated by means $\pm 1\sigma$ and posterior probability distributions. **D**, alternation of wet forest *Anomalopteryx didiformis* and alpine/glacial vegetation *P. australis* on Takaka Hill 15-9 ka BP, in relation to local $\delta^{18}\text{O}$ record, and GISP2 ice accumulation and methane. Black circles, *A. didiformis*; blue squares, *Pachyornis* spp.; green squares, *P. australis*; blue triangles, *Euryapteryx curtus*.

367



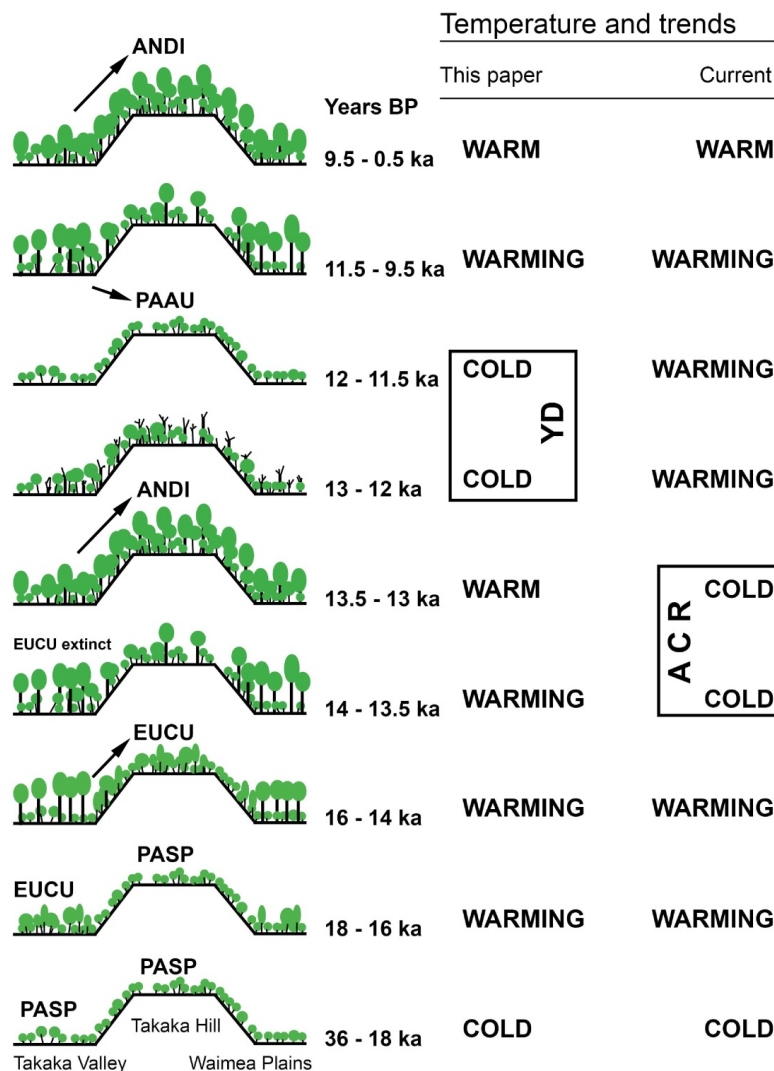
368
 369
 370
 371
 372
 373

Figure 10: Detail of integrated speleothem oxygen isotope record around the Mt Takaha (Antarctica) eruptions (Figure 3, panel C) at various LOESS smoothing factors, with dates of *Pachyornis australis* individuals collected from the Honeycomb Hill cave system deposits.



374
 375
 376
 377
 378

Figure 11: Detail of integrated speleothem oxygen isotope record around the Antarctic Cold Reversal and Younger Dryas periods (Figure 3, panel D) at various LOESS smoothing factors, with dates of *Anomalopteryx didiformis* and *Pachyornis australis* individuals collected from Takaka Hill cave deposits.



379

380 **Figure 12:** Comparison of present and proposed climatic contexts of changes in vegetation and moa populations
 381 around Takaka 36 - 0.5 ka BP. Arrows indicate direction of spread of taxon during that period (downward indicates
 382 movement from higher elevations to the south. YD, Younger Dryas; ACR, Antarctic Cold Reversal; other
 383 abbreviations as in Fig. 5.

384 **4 Discussion**



385 Unlike indirect proxies such as oxygen isotope ratios and pollen samples from a few sites, moa were on-ground
386 real-time witnesses to the vegetation (and hence climate) at the time and place they lived and died. The congruence
387 of the high spatial and temporal resolution record of vegetation based on ^{14}C ages of individual moa, each
388 characteristic of a particular vegetation (Fig. 12) with the local speleothem $\delta^{18}\text{O}$ record suggest that both proxies
389 accurately reflect the timing of changes in the New Zealand glacial and post-glacial climate. However, the post-
390 glacial return to cold climate in both records is later than the ACR. Instead, the moa sequence accords with the $\delta^{18}\text{O}$
391 record in showing that interval to be one of warming climate at these southern latitudes.

392 The cold interval recorded in the $\delta^{18}\text{O}$ and moa sequence on Takaka Hill, was coeval with the YD, when,
393 on the current model, the New Zealand climate should have been warming after the ACR. It is unlikely that there
394 are any significant issues with the moa radiocarbon ages which would affect their chronology because the ages from
395 different sites and measured by gas count and AMS provide coherent series.

396 In addition to the earlier evidence for a New Zealand YD presented by (Denton & Hendy, 1994) and (Ivy-
397 Ochs et al., 1999), more recently (Pauly et al., 2020) reported a return to cold climate in northern New Zealand
398 after the ACR, albeit of shorter duration. Stable isotope ratios in long-lived kauri (*Agathis australis*) trees reveal an
399 event that was brief relative to that in the north-western South Island. The difference may result from the trees'
400 being c. 5.5° (600 km) farther north, in an area surrounded by warm seas whose mild climate experiences, at least
401 today, few extremes of temperature (Chappell, 2013).

402 While the moa and speleothem $\delta^{18}\text{O}$ chronologies both support a cold period synchronous with the
403 European YD, neither provides any information that would help to resolve the difference between their chronologies
404 and those derived from cosmogenic glacial moraine dating or Antarctic ice cores. However, as a similar disparity
405 between chronologies exists with cosmogenically dated advances (or stability at greater extent) of the North
406 Patagonia Ice Field at 47°S contemporary with the YD (Glasser et al., 2012). Although (Glasser et al., 2012) posit
407 higher precipitation as an alternative to cooler temperatures as the driver of the Patagonian ice advances, this
408 explanation would not account for the vegetation changes signaled by the sequence of moa observed on TH.
409 Increased rainfall there would not have driven a return to glacial shrublands, which would have required a period of
410 intense cold. Until the differences between present chronologies are resolved, the interhemispheric postglacial
411 climatic seesaw model provides only one interpretation of global post-glacial climate processes.

412 The Oruanui eruption stands at the onset of the Last Glacial Maximum in the moa species sequence and in
413 the local $\delta^{18}\text{O}$ record. In addition to providing evidence for a Southern Hemisphere mid-latitude YD cold event, the



414 moa species sequence suggests that both the Oruanui super eruption of Taupo volcano (New Zealand) (Vandergoes
415 et al., 2013) affected the Southern Hemisphere climate. The climatic effects were sufficiently large to change the
416 vegetation pattern in the north-western South Island of New Zealand so that moa species changed their distributions.
417 The sudden appearance of *P. australis* at Honeycomb Hill immediately after the eruption means first that the species
418 was present in the area and second that there was a sudden increase in fossil deposition in the caves. That increase
419 may have resulted from an increase in local precipitation or from the removal of a pre-eruption vegetation cover and
420 its replacement by vegetation that was more susceptible to erosion.

421 (McConnell et al., 2017) suggested that the Mt Takahe eruption series in Antarctica may have initiated
422 post-glacial warming. In the moa species sequence, the eruption series marks a break in deposition of *P. australis* at
423 Honeycomb Hill. The break also coincides with a peak in the $\delta^{18}\text{O}$ record that began before the eruptions and which
424 declined rapidly after the eruptions. Instead, therefore, of the eruptions initiating the warming, they appear to have
425 stifled and reversed a warming trend, at least in central New Zealand. In initiating a cooling, these eruptions seem to
426 have had the same climatic effect of the much larger (VEI 8) – but much briefer – Oruanui eruption.

427 The patterns of moa species presence and absence west of New Zealand's South Island Main Divide appear
428 to provide a novel, valuable record of vegetation change over the past 30,000 years in a Southern Hemisphere
429 location athwart the mid-latitude westerlies. However, the patterns reported here were derived from published
430 radiocarbon ages measured for other purposes and not, therefore, aimed at providing complete chronologies for each
431 species in each site and each area. That coherent patterns are present that accord with the completely independent
432 climate proxy of speleothem $\delta^{18}\text{O}$ values suggests strongly the potential value of a concerted radiocarbon dating
433 programme of moa in developing a high resolution mid-latitude climate record for this most important, and
434 presently contentious, period.

435

436 5 Conclusions

- 437 • The patterns of presence and absence of habitat-specialist moa species in the north-western South Island of
438 New Zealand correspond to patterns in both an integrated multi-speleothem $\delta^{18}\text{O}$ record from the same area
439 and, significantly, in the Greenland GISP2 ice core proxies for the date of the European Younger Dryas.
- 440 • Neither the moa-based climate chronology nor that of the speleothem $\delta^{18}\text{O}$ values accords with that of the
441 Antarctic Cold Reversal.



- 442 • The present dichotomy in chronologies for post-glacial warming and cooling in the Southern Hemisphere
443 must be resolved before the interhemispheric postglacial climatic seesaw model can be accepted.
444 • More intensive, targeted radiocarbon dating of key moa species in the north-western South Island, New
445 Zealand will not only allow testing of the basis for the climate change chronology presented here, but could
446 provide a high precision chronology of climate in the region.

447

448

449 **6 Code availability**

450 No code was used.

451

452 **7 Data availability**

453 All data are included in the paper and the cited references.

454

455 **8 Author contributions**

456 RNH conceived the project, performed the analyses, drafted the figures, and prepared the manuscript.

457

458 **9 Competing interests**

459 The author declares that he has no conflict of interest.

460

461

462

463

464 **10 Acknowledgements**

465 Dr Richard Rowe (Research Associate, Australian National University) and Prof Don McFarlane (Claremont
466 Colleges, Los Angeles) provided helpful comments on the MS. There was no external funding for the study.

467

468

469

470

471



472 **11 References**

- 473 Allentoft, M. E., Heller, R., Oskam, C. L., Lorenzen, E. D., Hale, M. L., Gilbert, M. T., Jacomb, C., Holdaway, R.
474 N., and Bunce, M.: Extinct New Zealand megafauna were not in decline before human colonization,
475 Proceedings of the National Academy of Sciences, USA, 111, 4922-4927, 2014.
- 476 Barker, S., Diz, P., Vautravers, M. J., Pike, J., Knorr, G., Hall, I. R., and Broecker, W. S.: Interhemispheric Atlantic
477 seesaw response during the last deglaciation, Nature, 457, 1097-1102, 2009.
- 478 Broecker, W. S.: Paleocean circulation during the last deglaciation: a bipolar seesaw?, Paleoceanography, 13, 119-
479 121, 1998.
- 480 Brook, E. J., Sowers, T., and Orchardo, J.: Rapid variations in atmospheric methane concentration during the past
481 110,000 years, Science, 273, 1087-1091, 1996.
- 482 Bunce, M., Worthy, T. H., Phillips, M. J., Holdaway, R. N., Willerslev, E., Haile, J., Shapiro, B., Scofield, R. P.,
483 Drummond, A., Kamp, P. J., and Cooper, A.: The evolutionary history of the extinct ratite moa and New
484 Zealand Neogene paleogeography, Proceedings of the National Academy of Sciences U.S.A., 106, 20646-
485 20651, 2009.
- 486 Chappell, P. R. 2013 The climate and weather of Northland. 3 ed. Wellington: National Institute of Water and
487 Atmospheric Research.
- 488 Denton, G. H., and Hendy, C. t.: Younger Dryas age advance of Franz Josef glacier in the southern Alps of New
489 Zealand, Science, 264, 1434-1437, 1994.
- 490 Glasser, N. F., Harrison, S., Schnabel, C., Fabel, D., and Jansson, K. N.: Younger Dryas and early Holocene age
491 glacier advances in Patagonia, Quaternary Science Reviews, 58, 7-17, 2012.
- 492 Hajdas, I., Lowe, D. J., Newnham, R. M., and Bonani, G.: Timing of the late-glacial climate reversal in the Southern
493 Hemisphere using high-resolution radiocarbon chronology for Kaipo bog, New Zealand, Quaternary
494 Research, 65, 340-345, 2006.
- 495 Hammer, Ø., Harper, D. A. T., and Ryan, P. D.: PAST: Paleontological statistics software package for education
496 and data analysis, Palaeontologia electronica, 4, 9, 2001.
- 497 Hellstrom, J., McCulloch, M., and Stone, J.: A detailed 31,000-year record of climate and vegetation change, from
498 the isotope geochemistry of two New Zealand speleothems, Quaternary research, 50, 167-178, 1998.
- 499 Hogg, A., Heaton, T., Hua, Q., Bayliss, A., Blackwell, P., Boswijk, G., Ramsey, C., Palmer, J., Petchey, F., and
500 Reimer, P.: SHCal20 Southern Hemisphere calibration, 0–55,000 years cal BP, Radiocarbon, 62, 759-778,
501 2020.



- 502 Holdaway, R. N., Allentoft, M. E., Jacomb, C., Oskam, C. L., Beavan, N. R., and Bunce, M.: An extremely low-
503 density human population exterminated New Zealand moa, *Nature communications*, 5, 5436, 2014.
- 504 Holdaway, R. N., and Rowe, R. J.: Palaeoecological reconstructions depend on accurate species identification:
505 examples from South Island, New Zealand, *Pachyornis* (Aves: Dinornithiformes), *Notornis*, 67, 494-502,
506 2020.
- 507 Holdaway, R. N., and Worthy, T. H.: A reappraisal of the late Quaternary fossil vertebrates of Pyramid Valley
508 Swamp, North Canterbury, New Zealand, *New Zealand Journal of Zoology*, 24, 69-121, 1997.
- 509 Huynen, L., Gill, B. J., Doyle, A., Millar, C. D., and Lambert, D. M.: Identification, classification, and growth of
510 moa chicks (Aves: Dinornithiformes) from the genus *Euryapteryx*, *PLoS One*, 9, e99929, 2014.
- 511 Huynen, L., Gill, B. J., Millar, C. D., and Lambert, D. M.: Ancient DNA reveals extreme egg morphology and
512 nesting behavior in New Zealand's extinct moa, *Proceedings of the National Academy of Sciences*, 107,
513 16201-16206, 2010.
- 514 Ivy-Ochs, S., Schlüchter, C., Kubik, P. W., and Denton, G. H.: Moraine exposure dates imply synchronous Younger
515 Dryas glacier advances in the European Alps and in the Southern Alps of New Zealand, *Geografiska*
516 *Annaler: Series A, Physical Geography*, 81, 313-323, 1999.
- 517 Kaplan, M. R., Schaefer, J. M., Denton, G. H., Barrell, D. J., Chinn, T. J., Putnam, A. E., Andersen, B. G., Finkel,
518 R. C., Schwartz, R., and Doughty, A. M.: Glacier retreat in New Zealand during the Younger Dryas stadial,
519 *Nature*, 467, 194, 2010.
- 520 Koffman, T. N., Schaefer, J. M., Putnam, A. E., Denton, G. H., Barrell, D. J., Rowan, A. V., Finkel, R. C., Rood, D.
521 H., Schwartz, R., and Plummer, M. A.: A beryllium-10 chronology of late-glacial moraines in the upper
522 Rakaia valley, Southern Alps, New Zealand supports Southern-Hemisphere warming during the Younger
523 Dryas, *Quaternary Science Reviews*, 170, 14-25, 2017.
- 524 Lowe, D. J., and Hogg, A. G.: Tephrostratigraphy and chronology of the Kaipo Lagoon, an 11,500 year-old
525 montane peat bog in Urewera National Park, New Zealand, *Journal of the Royal Society of New Zealand*,
526 16, 25-41, 1986.
- 527 Mabin, M., Denton, G., and Hendy, C.: The age of the Waiho Loop glacial event, *Science*, 271, 668-670, 1996.
- 528 McConnell, J. R., Burke, A., Dunbar, N. W., Köhler, P., Thomas, J. L., Arienzo, M. M., Chellman, N. J., Maselli,
529 O. J., Sigl, M., and Adkins, J. F.: Synchronous volcanic eruptions and abrupt climate change~ 17.7 ka
530 plausibly linked by stratospheric ozone depletion, *Proceedings of the National Academy of Sciences*, 114,
531 10035-10040, 2017.



- 532 Meese, D. A., Gow, A., Grootes, P., Stuiver, M., Mayewski, P. A., Zielinski, G., Ram, M., Taylor, K., and
533 Waddington, E.: The accumulation record from the GISP2 core as an indicator of climate change
534 throughout the Holocene, *Science*, 266, 1680-1682, 1994.
- 535 Newnham, R.: Temperature Changes During the Younger Dryas in New Zealand, *Science*, 283, 759-759, 1999.
- 536 Oppenheimer, C.: Eruptions that shook the world, Cambridge University Press, Cambridge, 2011.
- 537 Pauly, M., Turney, C., Palmer, J., Büntgen, U., Brauer, A., and Helle, G.: Kauri tree-ring stable isotopes reveal a
538 centennial climate downturn following the Antarctic Cold Reversal in New Zealand, *Geophysical Research*
539 *Letters*, e2020GL090299, 2020.
- 540 Putnam, A. E., Denton, G. H., Schaefer, J. M., Barrell, D. J., Andersen, B. G., Finkel, R. C., Schwartz, R., Doughty,
541 A. M., Kaplan, M. R., and Schlüchter, C.: Glacier advance in southern middle-latitudes during the
542 Antarctic Cold Reversal, *Nature Geoscience*, 3, 700, 2010.
- 543 Ramsey, C. B.: Radiocarbon calibration and analysis of stratigraphy: the OxCal program, *Radiocarbon*, 37, 425-
544 430, 1995.
- 545 Ramsey, C. B.: Bayesian analysis of radiocarbon dates, *Radiocarbon*, 51, 337-360, 2009.
- 546 Rawlence, N. J., and Cooper, A.: Youngest reported radiocarbon age of a moa (*Aves: Dinornithiformes*) dated from
547 a natural site in New Zealand, *Journal of the Royal Society of New Zealand*, 43, 100-107, 2013.
- 548 Rawlence, N. J., Metcalf, J. L., Wood, J. R., Worthy, T. H., Austin, J. J., and Cooper, A.: The effect of climate and
549 environmental change on the megafaunal moa of New Zealand in the absence of humans, *Quaternary*
550 *science reviews*, 50, 141-153, 2012.
- 551 Rawlence, N. J., Scofield, R. P., Wood, J. R., Wilmshurst, J. M., Moar, N. T., and Worthy, T. H.: New
552 palaeontological data from the excavation of the Late Glacial Glencrieff miring bone deposit, North
553 Canterbury, South Island, New Zealand, *Journal of the Royal Society of New Zealand*, 41, 217-236, 2011.
- 554 Shulmeister, J., Fink, D., and Augustinus, P. C.: A cosmogenic nuclide chronology of the last glacial transition in
555 North-West Nelson, New Zealand—new insights in Southern Hemisphere climate forcing during the last
556 deglaciation, *Earth and Planetary Science Letters*, 233, 455-466, 2005.
- 557 Singer, C., Shulmeister, J., and MeLea, B.: Evidence against a significant Younger Dryas cooling event in New
558 Zealand, *Science*, 281, 812-814, 1998.
- 559 Tovar, D. S., Shulmeister, J., and Davies, T.: Evidence for a landslide origin of New Zealand's Waiho Loop
560 moraine, *Nature Geoscience*, 1, 524-526, 2008.



- 561 Vandergoes, M. J., Hogg, A. G., Lowe, D. J., Newnham, R. M., Denton, G. H., Southon, J., Barrell, D. J., Wilson,
562 C. J., McGlone, M. S., and Allan, A. S.: A revised age for the Kawakawa/Oruanui tephra, a key marker for
563 the Last Glacial Maximum in New Zealand, *Quaternary Science Reviews*, 74, 195-201, 2013.
- 564 Williams, P. W., King, D., Zhao, J.-X., and Collerson, K.: Late Pleistocene to Holocene composite speleothem 18O
565 and 13C chronologies from South Island, New Zealand—did a global Younger Dryas really exist?, *Earth
566 and Planetary Science Letters*, 230, 301-317, 2005.
- 567 Williams, P. W., Neil, H. L., and Zhao, J.-X.: Age frequency distribution and revised stable isotope curves for New
568 Zealand speleothems: palaeoclimatic implications, *International Journal of Speleology*, 39, 5, 2010.
- 569 Worthy, T. H.: Validation of *Pachyornis australis* Oliver (Aves; Dinornithiformes), a medium sized moa from the
570 South Island, New Zealand, *New Zealand journal of geology and geophysics*, 32, 255-266, 1989.
- 571 Worthy, T. H.: Fossils of Honeycomb Hill, Museum of New Zealand Te Papa Tongarewa, Wellington, New
572 Zealand, 1993a.
- 573 Worthy, T. H.: Submarine fossil moa bones from the northern South Island, *Journal of the Royal Society of New
574 Zealand*, 23, 255-256, 1993b.
- 575 Worthy, T. H.: Fossil deposits in the Hodges Creek Cave System, on the northern foothills of Mt Arthur, Nelson.
576 South Island, New Zealand, *Notornis*, 44, 111-108, 1997.
- 577 Worthy, T. H.: Two late-Glacial avifaunas from eastern North Island, New Zealand-Te Aute Swamp and Wheturau
578 Quarry, *Journal of the Royal Society of New Zealand*, 30, 1-25, 2000.
- 579 Worthy, T. H.: Rediscovery of the types of *Dinornis curtus* Owen and *Palapteryx geranoides* Owen, with a new
580 synonymy (Aves: Dinornithiformes), *Tuhinga*, 16, 57-67, 2005.
- 581 Worthy, T. H., and Holdaway, R. N.: Quaternary fossil faunas from caves in the Punakaiki area, West Coast, South
582 Island, New Zealand, *Journal of the Royal Society of New Zealand*, 23, 147-254, 1993.
- 583 Worthy, T. H., and Holdaway, R. N.: Quaternary fossil faunas from caves in Takaka valley and on Takaka Hill,
584 northwest Nelson, South Island, New Zealand, *Journal of the Royal Society of New Zealand*, 24, 297-391,
585 1994.
- 586 Worthy, T. H., and Holdaway, R. N.: Quaternary fossil faunas from caves on Mt Cookson, North Canterbury, South
587 Island, New Zealand, *Journal of the Royal Society of New Zealand*, 25, 333-370, 1995.
- 588 Worthy, T. H., and Holdaway, R. N.: Quaternary fossil faunas, overlapping taphonomies, and palaeofaunal
589 reconstruction in North Canterbury, South Island, New Zealand, *Journal of the Royal Society of New
590 Zealand*, 26, 275-361, 1996.



- 591 Worthy, T. H., and Holdaway, R. N.: Lost world of the moa: prehistoric life in New Zealand, Indiana University
592 Press and Canterbury University Press, Bloomington and Christchurch, 2002.
- 593 Worthy, T. H., and Roscoe, D.: Takaka Fossil Cave: a stratified Late Glacial to Late Holocene deposit from Takaka
594 Hill, New Zealand, Tuhinga, 41-60, 2003.
- 595
- 596